Acta Mech
https://doi.org/10.1007/s00707-018-2246-8

ORIGINAL PAPER

Nina Čeh · Gordan Jelenić · Nenad Bićanić

Analysis of restitution in rocking of single rigid blocks

Received: 20 March 2018 / Revised: 9 August 2018

Abstract A single rigid prismatic block is analysed for free rocking behaviour without sliding and jumping. A numerical procedure based on a precise contact detection is developed and tested. An extensive experimental study of free rocking for blocks of different slenderness and size is conducted, with the emphasis on the post-impact behaviour and energy loss mechanism in the existing impact models. The experiments conducted strongly support the definition of the restitution coefficient proposed both by Kalliontzis et al. (J Struct Eng 142(12):06016002, 2016) and by Chatzis et al. (J Eng Mech 143(5):04017013, 2017). A method is proposed to determine the extra parameter present in this model.

1 Introduction

Free and forced rocking is a vitally important mode of motion which needs to be properly understood in the analysis of historical structures (such as monuments or dry stone walls, where multiple rigid bodies are freely standing one on top of another), graphite cores inside nuclear power plants (which consist of a large number of rigid bodies deliberately designed with gaps and clearances between them so that thermal expansion is possible), or masonry structural elements after the failure of the binding component. Controlled rocking can also be a practical alternative for seismic isolation of tall slender structures [11]. For these reasons, rocking motion of simple small-scale models has to be scrutinised in detail so that a better understanding of it is achieved and then applied to more complex structures.

In-plane rocking of rigid prismatic blocks was first addressed by Housner [7]. He derived the nonlinear equation of motion of the block standing on a rigid base with a single degree of freedom—the angle of rotation. He assumed that for slender blocks a linearised equation of motion is still appropriate and derived the analytical solutions for what he called the 'period and frequency of rocking motion', which turned out to be dependent on the initial conditions. Following Housner's work, the analytical condition for initiation of rocking and the minimum ground acceleration of a specific acceleration function necessary for overturning have been further derived from the linearised equation of motion [7,13,14,19,21,23], while the fully nonlinear equation of motion using the state-space procedure and built-in ODE solvers has been analysed in [5,12–14,23]. In the literature, rocking has been also modelled so that the elasticity of the rocking block itself or, more often, the ground is accounted for; see, e.g., [10,20] and the references therein. Clearly, while in these models we still deal with a discontinuous contact-dynamics problem, the contact duration becomes protracted, and thus, we avoid singularities in the contact forces associated with a finite impulse, which is clearly beneficial in simulations. On the other hand, such models necessarily involve strain energy in a problem with a potential

Nenad Bićanić: Deceased

N. Čeh · G. Jelenić (✉)
Faculty of Civil Engineering, University of Rijeka, Radmile Matejčić 3, 51000 Rijeka, Croatia
E-mail: gordan.jelenic@uniri.hr
Tel.: +385-51-265-955

Published online: 11 September 2018

energy so far completely given only by its gravitational part. From the point of view of simulation, this presents an added complexity, possibly leading to a problem of integrating stiff contact-dynamics problems, in which higher-mode oscillations need to be properly resolved.

Even though the equations of motion for a single rigid rectangular block have been presented more than 50 years ago, the topic still exposes some unanswered question and is being addressed more in the past few years (see [5,11] among others). One of them is the question of how to properly account for the energy loss at the time when the instant centre of rotation shifts from one corner of the block to the other.

The classical Housner's approach accounts for such energy loss by means of a coefficient of restitution following an angular momentum balance around the new centre of rotation assumed to stay in contact with the ground [7]. The experimental studies of the coefficient of restitution in rocking, however, have resulted in a large scatter and the values repeatedly larger than Housner's [2,3,6,9,15–18].

The researchers have continued questioning the accuracy of Housner's impact model, so a new improved restitution model has been presented very recently independently by two research groups: Kalliontzis et al. [8] and Chatzis et al. [4]. While Housner's impact model is in good agreement with the experimental results when the contact point after the impact is forced to be at the very corner of the block, the impact model presented in [4,8] shows better agreement with experimental results when the position of the contact point is unknown, such as in flat-base blocks.

In this work, we carry on with these studies and address free rocking of single rigid prismatic blocks with a view on investigating the energy loss mechanism by developing a suitable numerical and carefully designed experimental approach simultaneously. Only the situations in which the block cannot slide along the base or detach from it and jump during rocking are considered in this work.

The numerical time-stepping scheme is specifically developed with a contact detection algorithm designed to satisfy the angular momentum balance.

The numerical procedure developed is then compared against the experimental results, where a specially designed experimental programme is devised along with the method to eliminate sliding and prescribe various controlled initial conditions.

2 Problem description

A rigid prismatic block of mass m, rectangular base of unit thickness, width b and height h (or the half-diagonal R of its frontal side and the angle of slenderness $\alpha = \tan^{-1}\frac{b}{h}$) lies on a rigid base platform and is either initially tilted or is subject to a prescribed horizontal ground acceleration function of arbitrary type. We address the case whereby sliding between the block and the ground is prevented, and it is assumed that contact between the block and the ground is maintained throughout the motion. The most important practical question is whether, for a prescribed set of input parameters such as geometry of the block and shape and parameters of the prescribed ground acceleration function, the block will translate with the ground, rock in a stable fashion or overturn. The specific case we address here is a simple free rocking with no ground motion, which is particularly suitable if we want to focus only on the contact-induced energy loss.

In general, rotational motion of the block around one of its bottom corners (either corner A or corner B) is initiated by ground acceleration $\ddot{u}$ when $\ddot{u} > g\tan\alpha$ with g as the constant of gravity.

Such behaviour is described with a set of equations of motion derived from Fig. 1 as

$$I_A\ddot{\theta} + mgR\sin(\alpha-\theta) + m\ddot{u}R\cos(\alpha-\theta) = 0 \quad \text{if} \quad \theta > 0, \tag{1}$$

$$I_A\ddot{\theta} - mgR\sin(\alpha+\theta) + m\ddot{u}R\cos(\alpha+\theta) = 0 \quad \text{if} \quad \theta < 0, \tag{2}$$

with θ as the angle of rotation, m as the mass of the block and $I_A = \frac{4}{3}mR^2$ as its moment of inertia around either of the contact points, while the superimposed dots here and in Fig. 1 indicate time differentiation.

In analogy with a forced harmonic oscillator Housner defined the so-called frequency parameter of rocking motion as $p = \sqrt{\frac{mgR}{I_A}} = \sqrt{\frac{3g}{4R}}$ [7]. In case of free rocking $\ddot{u} = 0$ and Eqs. (1) and (2) become

$$\ddot{\theta} + p^2\sin(\alpha-\theta) = 0 \quad \text{if} \quad \theta > 0, \tag{3}$$

$$\ddot{\theta} - p^2\sin(\alpha+\theta) = 0 \quad \text{if} \quad \theta < 0. \tag{4}$$

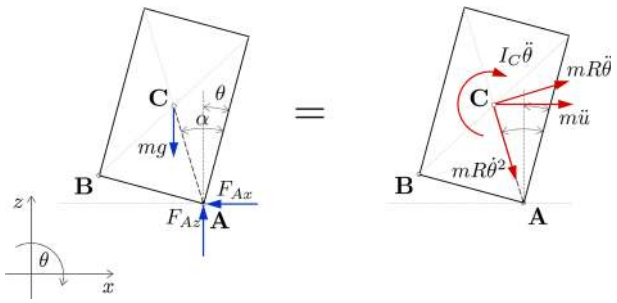

Fig. 1 Free-body and mass–acceleration diagrams during rotation of a single rigid rectangular block

3 Numerical analysis and contact treatment

Equations (3) and (4) will be integrated numerically using the well-known Newmark's trapezoidal time-stepping rule [22] at discrete time instants separated by the time step Δt, in which $\ddot{\theta}\,(t_n + \Delta t)$ is given in terms of $\theta\,(t_n)$, $\dot{\theta}\,(t_n)$, $\ddot{\theta}\,(t_n)$ and $\theta\,(t_n + \Delta t)$ as

$$\ddot{\theta}_{n+1} = \frac{\theta_{n+1} - \theta_n}{\beta \Delta t^2} - \frac{1}{\beta \Delta t}\dot{\theta}_n - \frac{\frac{1}{2} - \beta}{\beta}\ddot{\theta}_n, \quad \dot{\theta}_{n+1} = \Delta t\left[(1-\gamma)\ddot{\theta}_n + \gamma \ddot{\theta}_{n+1}\right] + \dot{\theta}_n \tag{5}$$

with β and γ as the integration parameters, in this work taken as $\beta = \frac{1}{4}$ and $\gamma = \frac{1}{2}$ (the trapezoidal rule). The nonlinear algebraic equations of motion thus obtained,

$$4\frac{\theta_{n+1} - \theta_n}{\Delta t^2} - \frac{4}{\Delta t}\dot{\theta}_n - \ddot{\theta}_n + p^2 \sin(\alpha - \theta_{n+1}) = 0 \quad \text{if} \quad \theta_n, \theta_{n+1} > 0, \tag{6}$$

$$4\frac{\theta_{n+1} - \theta_n}{\Delta t^2} - \frac{4}{\Delta t}\dot{\theta}_n - \ddot{\theta}_n - p^2 \sin(\alpha + \theta_{n+1}) = 0 \quad \text{if} \quad \theta_n, \theta_{n+1} < 0, \tag{7}$$

are solved iteratively using the Newton–Raphson solution procedure for θ_{n+1} at every time step. To make the transition from one of the equations of motion to the other, which occurs when the block impacts the base without any constraint violation, it becomes important to detect the time of the contact precisely. Such treatment of the contact belongs to the event-tracking time-stepping schemes which are based on accurate detection of contacts (see, e.g., [1]). The use of these schemes is justified in cases when a relatively small number of contacts is expected, such as rocking of a system consisting of a small number of blocks, where there is no risk of numerical inefficiency. At the same time, such contact treatment enables a detailed analysis of the energy loss mechanism during contact.

3.1 Contact detection and resolution

We propose a technique in which the rotation at the end of a time step is monitored throughout the analysis for the change of sign. When such change is detected, so that at a time t_{n+1} either $\theta_n > 0$ and $\theta_{n+1} < 0$ or $\theta_n < 0$ and $\theta_{n+1} > 0$, the dynamic equilibrium over the time step is repeated for an *unknown modified time-step length* $\Delta t'$ under the condition that $\theta_{n+1} := 0$, i.e., the following equation (obtained from Eqs. (3) and (4) written at time instant $n + 1$ taking into account the condition for zero rotation)

$$A\Delta t'^2 - 4\dot{\theta}_n \Delta t' - \theta_n = 0 \tag{8}$$

needs to be solved for the unknown $\Delta t'$, where $A = p^2 \sin\alpha - \ddot{\theta}_n$ for $\theta_n > 0$ or $A = -p^2 \sin\alpha - \ddot{\theta}_n$ for $\theta_n < 0$. Let us emphasise the fact that this equation is written for the case of free rocking ($\ddot{u} = 0$) and is quadratic with respect to the unknown $\Delta t'$ only owing to the fact that there is no ground acceleration. If a ground acceleration were present, this equation would cease to be quadratic and would have to be solved iteratively. In the present case, since θ_n and θ_{n+1} are of opposite signs, there must exist one and only one root within $[0, \Delta t]$ the other

root of necessity therefore also being real. Since, prior to the contact, θ_n and $\dot{\theta}_n$ are always of opposite signs the required root always follows as

$$\Delta t' = \frac{2}{A}\left(\dot{\theta}_n + \sqrt{\dot{\theta}_n^2 + A\theta_n}\right). \tag{9}$$

Once the modified time step size is calculated, the pre-impact (for time $t^- = t_n + \Delta t'$) angular velocity $\dot{\theta}^-$, and angular acceleration $\ddot{\theta}^-$ are calculated using Newmark's trapezoidal rule as

$$\dot{\theta}^- = \frac{2}{\Delta t'}(0 - \theta_n) - \dot{\theta}_n, \tag{10}$$

$$\ddot{\theta}^- = \frac{4}{\Delta t'^2}(0 - \theta_n) - \frac{4}{\Delta t'}\dot{\theta}_n - \ddot{\theta}_n. \tag{11}$$

After the impact, the original time-step length Δt is restored and the time-stepping procedure switches to the other equation of motion. Before proceeding, however, the angular velocity at the beginning of the first post-impact time step has to be determined.

3.2 Housner's original impact description

Housner proposed that when the exact time of the impact is detected, the angular velocity $\dot{\theta}^+$ immediately after the contact should be reduced with respect to that immediately before the contact ($\dot{\theta}^-$) following the angular momentum balance with respect to the new contact point as [7]

$$\dot{\theta}^+ = \left(1 - \frac{3}{2}\sin^2\alpha\right)\dot{\theta}^-. \tag{12}$$

The angular acceleration $\ddot{\theta}^+$ should follow from the corresponding equation of motion for the post-impact pattern of motion.

It is convenient to take the new contact point (point B in Fig. 1) as the reference point with respect to which the angular momentum of the system is conserved because all the impulses act in this point, and all other forces (such as weight of the block and contact forces of finite value) result in zero impulse for $t^+ - t^- \to 0$.

It is interesting to notice that even when there is no energy loss due to material dissipation, the total mechanical energy (i.e., the kinetic energy) is not conserved during the impact and a real coefficient of restitution defined as the ratio between the post-impact and the pre-impact angular velocity can never exceed Housner's [7] value

$$\eta_{\mathrm{H}} = 1 - \frac{3}{2}\sin^2\alpha < 1. \tag{13}$$

Note that here we define a restitution coefficient as a ratio between the post-impact and pre-impact velocities, and not as the ratio between the post-impact and pre-impact kinetic energies (equivalent to the ratio between squares of the post-impact and pre-impact velocities). The fact that $\eta_{\mathrm{H}} < 1$ makes pure rocking as described by Housner (i.e., such that there is no sliding and no detachment from the ground) inherently a non-conservative mechanical problem. Let us emphasise that Housner's coefficient of restitution is purely a geometric property and can be a priori calculated for each block when there is no material dissipation. Its value is shown in Fig. 3 with respect to block's slenderness ratio. The experimentally obtained results available in the literature [2,3,6,9,15–18], however, show that Housner's model clearly underestimates the actual coefficient of restitution and thus overestimates the stability of the block, see also Fig. 3.

3.3 Modified impact description

Recently, in order to improve Housner's prediction, Kalliontzis et al. [8] and Chatzis et al. [4] have independently considered the possibility that the resultant impulses during impact between the block and the base during rocking act at some point between the bottom corners of the block, rather than at the corners as assumed

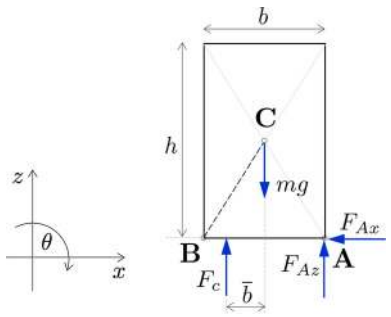

Fig. 2 Free-body diagram of the model due to Kalliontzis et al. [8] and Chatzis et al. [4] at the time of impact following rotation around corner *A*

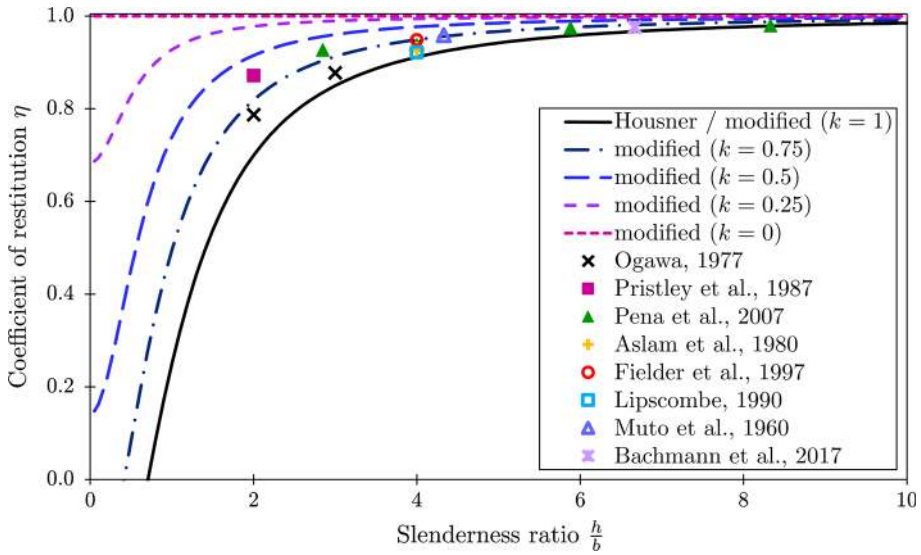

Fig. 3 Coefficient of restitution from Housner's formula [7], modified formula [4,8] and previous experiments [2,3,6,9,15–18]

by Housner. They have both thus proposed an improved formula to calculate the coefficient of restitution. The modified formula followed in this work

$$\eta_{\mathrm{M}} = \frac{4 - 3\sin^2\alpha\left(1 + k^2\right)}{4 - 3\sin^2\alpha\left(1 - k^2\right)} \tag{14}$$

is given in [8], although the same formula with slightly different notation is also given in [4]. In the above formula $k = \frac{2\overline{b}}{b}$, and $\overline{b}$ is the distance between the middle of the block and the point at which the resultant impulse acts as shown in Fig. 2, where F_c is the resultant impact force. The restitution coefficient obtained in this way is shown with respect to block's slenderness $\frac{h}{b}$ for four different values of k in Fig. 3. Housner's coefficient of restitution is, therefore, a special case in the improved description when $k = 1$.

Obviously the improved restitution coefficient is in better agreement with the experimental results, especially for the stockier blocks. The improved restitution coefficient is universally applicable for blocks of different slendernesses, even though Housner's restitution is closer to experimentally obtained results for very slender blocks. To this day, there does not exist a plausible proposal of how to estimate the extra parameter in the model. We will make such a proposal in Sect. 5.4 based on the analysis of the experiments conducted in Sects. 5.1 and 5.2.

3.4 Numerical algorithm

A numerical algorithm following the explained approach is shown graphically in Fig. 4.

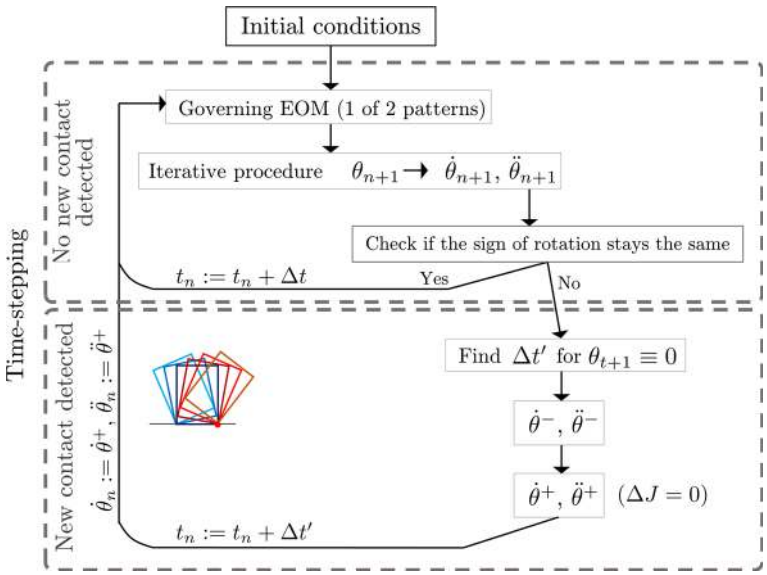

Fig. 4 Algorithm for simulation of rocking of a rigid prismatic block

Table 1 Geometric characteristics, coefficient of restitution and post-impact behaviour of the numerically tested blocks

Block	Geometry					η_H [7]	Behaviour
	b (m)	h (m)	$\frac{h}{b}$	α (rad)	R (m)		
$B1_N$	0.03	0.135	4.5	0.2187	0.0691	0.9294	Rocking
$B2_N$	0.03	0.045	1.5	0.5880	0.0270	0.5385	Rocking

The algorithm is able to reproduce the three physically attainable post-impact patterns of motion for the analysed case in which no sliding and no detachment from the ground are allowed (rocking, bouncing back and staying still) depending on the geometrical parameters of the block. Let us emphasise that the two non-rocking patterns should be considered only as an artefact of the model analysed in this work. In reality, for blocks with geometry resulting in these patterns (relatively stocky blocks), the assumption that there is no sliding and no detachment from the ground becomes hardly tenable. For presentation purposes, two realistic cases of different blocks with $\eta_H > 0$, i.e., $\frac{h}{b} > \frac{1}{\sqrt{2}}$, are analysed using the described numerical procedure (blocks $B1_N$ and $B2_N$). The geometry, restitution coefficient and behaviour type of the two blocks are shown in Table 1, while the normalised rotation, the angular velocity and the energy time histories of the blocks are shown in Fig. 5. The energy of the block is calculated as

$$E = I_C\dot{\theta}^2 + \frac{m}{2}R^2\dot{\theta}^2 + mg\left[R\cos(\alpha \pm \theta) - \frac{h}{2}\right]. \tag{15}$$

Results from the numerical simulations show that the blocks carry on rocking after they have impacted the base, where higher slenderness is related to higher η_H, i.e., lower energy dissipation. The same behaviour can be observed from the jumps in the velocity time histories.

Such numerical algorithm enables for the material dissipation occurring during the impact to be included additionally.

4 Experimental set-up

An extensive experimental programme has been designed aiming to investigate the energy loss mechanism in free rocking. The emphasis has been put on examining the coefficient of restitution and overall post-impact behaviour with respect to slenderness and scale of the block as well as the contact conditions between the block and the base.

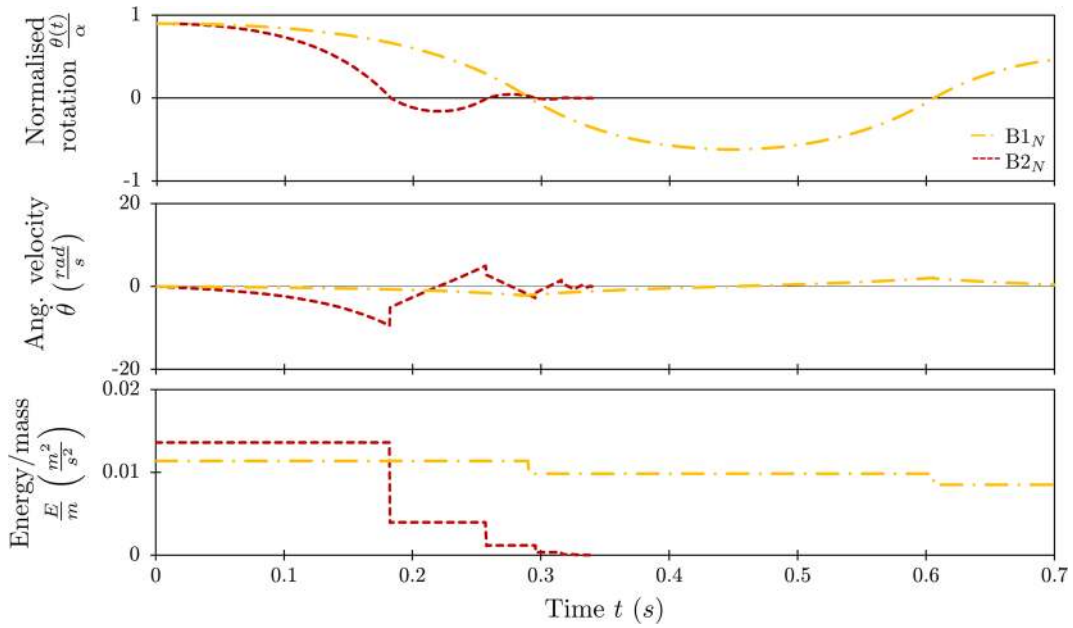

Fig. 5 Rotation and angular velocity time histories obtained from numerical algorithm for two different geometries of a single block without material dissipation

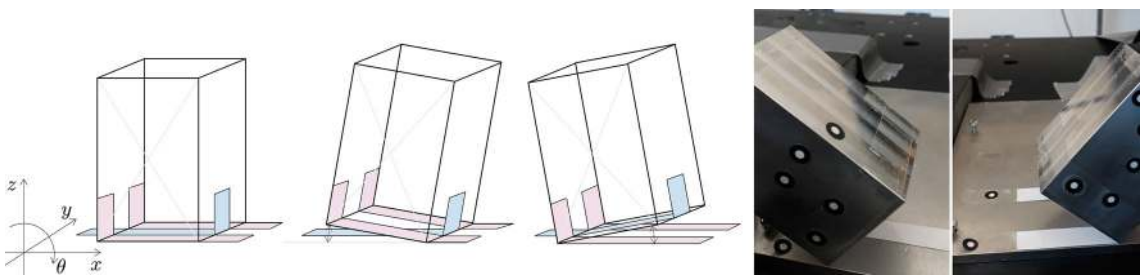

Fig. 6 System of tapes designed to avoid sliding and/or jumping of the block on the base

4.1 Sample preparation

The blocks of ten different slenderness ratios $\frac{h}{b}$ (B1–B10) on three different scales (S—small, M—medium, L—large) have been used as samples in the experimental programme, and their properties are shown in Table 2. Thickness of all the blocks is equal to their width apart from blocks B1, which have larger thickness. All the blocks are made of aluminium.

To prevent sliding and jumping as well as any out-of-plane motion of the blocks during testing a system of very thin tapes (a paper strip sandwiched between two *sellotape* adhesive tapes) attached to both the samples and the base beneath them is used (Fig. 6). In this way, only rocking or bouncing back of the block is enabled. The tapes provide virtually no rotational resistance during rocking.

To investigate the effect of the correction of Housner's restitution coefficient due to Kalliontzis et al. [8] and Chatzis et al. [4] two different sets of contact conditions—full contact and edge contact—are designed as shown in Fig. 7. In the full-contact set-up, the actual point of impact between the block and the base is fully unknown, while in the edge-contact set-up this point is bound to be in the narrow region (here $l_c = 1.5\,\text{mm}$ wide) near the edges of the block. A related idea of modifying the block in order to make Housner's assumption for the position of impact impulse more accurate is suggested in [4].

4.2 Initiation of free rocking

The free rocking is initiated by setting the block into an initially tilted position (such that the initial rotation θ_0 is not greater than the block's angle of slenderness α) with zero initial angular velocity, and releasing it. The

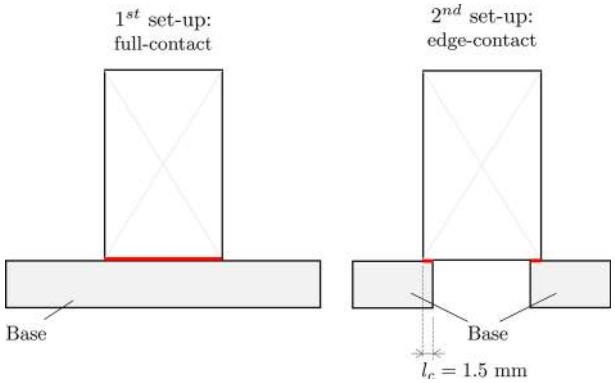

Fig. 7 Two experimental set-ups with different contacts between the block and the base

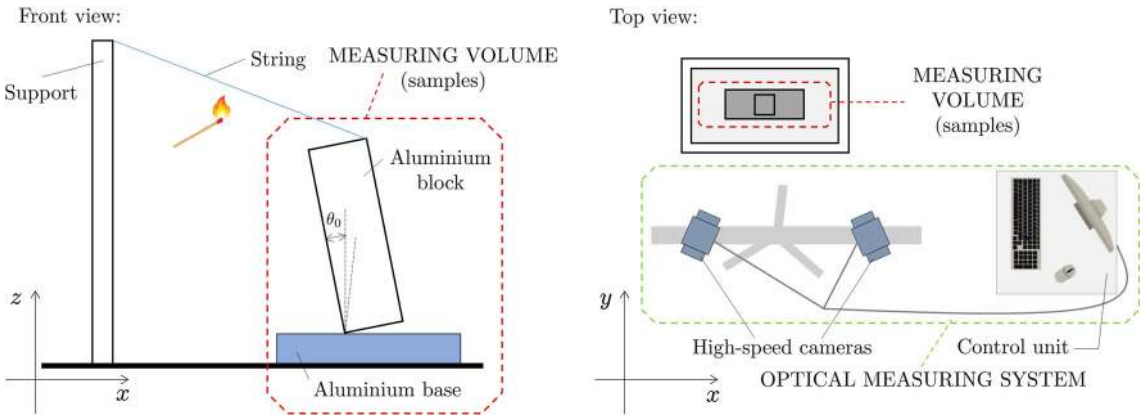

Fig. 8 Free rocking experimental set-up and measuring system: block in its tilted initial position (left) and top view showing the position of the measuring system (right)

condition of zero initial velocity is provided by designing a special release system: the initially tilted block, connected to the base with a set of tapes described in the previous section and to another body with a piece of string, is set in motion by burning the string at the beginning of the experiment (Fig. 8). Cutting the string by hand, alternatively, using a pair of scissors would in practice inevitably introduce unwanted perturbation and an initial velocity. With the motion initiated as described, post-processing the measured velocities reveals that the string breaks without any extension while it burns which, if present, would spoil the condition of the zero initial angular velocity required. Setting the block in motion in this way is inspired by the so-called *thread-burn start* sometimes used in Foucault's pendula with the aim of providing transversal-velocity-free initial conditions needed to minimise the spurious spherical precession.

4.3 Measurement

Motion of the samples is monitored using the 3D contactless optical measuring system GOM Pontos (version 6.3 and 8.0). The system comprises a set of two high-speed full-resolution cameras, an acquisition unit and post-processing software Pontos. The system is shown inside a green dashed line on the right in Fig. 8. Every experiment is filmed in full resolution (2400 × 1728 pixels) with 150 frames-per-second (fps) frequency. The positions of the testing samples in time (including the initial position) are obtained by post-processing the videos from the experiments. The initial rotation obtained in this way is then given as an input for the numerical simulation described in the previous section.

Table 2 Geometric characteristics and masses of the tested blocks

Block	m (g)	b (m)	h (m)	$\frac{h}{b}$	α (rad)	R (m)
B1S	113.3	0.03	0.03	1	0.7854	0.0212
B2S	113.3	0.03	0.045	1.5	0.5880	0.0270
B3S	161.2	0.03	0.0675	2.25	0.4182	0.0369
B4S	226.6	0.03	0.09	3	0.3218	0.0474
B5S	274.5	0.03	0.1125	3.75	0.2606	0.0582
B6S	339.6	0.03	0.135	4.5	0.2187	0.0691
B7S	453.2	0.03	0.18	6	0.1651	0.0912
B8S	500.8	0.03	0.2025	6.75	0.1471	0.1024
B9S	614.1	0.03	0.2475	8.25	0.1206	0.1247
B10S	727.4	0.03	0.2925	9.75	0.1022	0.1470
B1M	363.6	0.045	0.045	1	0.7854	0.0318
B2M	363.6	0.045	0.0675	1.5	0.5880	0.0406
B3M	544.4	0.045	0.10125	2.25	0.4182	0.0554
B4M	727.2	0.045	0.135	3	0.3218	0.0712
B5M	907.7	0.045	0.16875	3.75	0.2606	0.0873
B6M	1089.6	0.045	0.2025	4.5	0.2187	0.1037
B7M	1453.2	0.045	0.27	6	0.1651	0.1369
B8M	1634.0	0.045	0.30375	6.75	0.1471	0.1535
B9M	1997.6	0.045	0.37125	8.25	0.1206	0.1870
B10M	2361.2	0.045	0.43875	9.75	0.1022	0.2205
B1L	856.6	0.06	0.06	1	0.7854	0.0424
B2L	856.6	0.06	0.09	1.5	0.5880	0.0541
B3L	1284.3	0.06	0.135	2.25	0.4182	0.0739
B4L	1713.2	0.06	0.18	3	0.3218	0.0949
B5L	2140.9	0.06	0.225	3.75	0.2606	0.1164
B6L	2569.2	0.06	0.27	4.5	0.2187	0.1383
B7L	3425.8	0.06	0.36	6	0.1651	0.1825
B8L	3853.5	0.06	0.405	6.75	0.1471	0.2047
B9L	4710.1	0.06	0.495	8.25	0.1206	0.2493
B10L	5566.7	0.06	0.585	9.75	0.1022	0.2940

5 Results and analysis

The time histories from each experiment are compared to the time histories from the numerical simulation for the block with the same geometry and initial conditions. The coefficient of restitution initially used in the numerical simulations is η_{H} [7] and η_{M} [4,8], as given in Eqs. (13) and (14).

This experiment is designed to question the conditions for rocking and the relation between η_{H}, η_{M} and the actual restitution in the physical model. The effects of slenderness and size, as well as the effect of different contacts between the block and the base to the restitution, are investigated.

5.1 Full-contact experiments

First, the results obtained using Housner's restitution for three representative blocks from the group of blocks 0.045 m wide (medium scale) spanning the full range of possible slendernesses (blocks B2M, B6M and B10M in Table 2) are shown in Fig. 9.

Post-impact rocking is both observed experimentally and computed numerically. Given that no material dissipation is included in the computation of η_{H}, we would expect that the experimentally obtained amplitudes should be smaller than those from the numerical simulation, and, correspondingly, that the periods from the experiment should be also smaller than those from the simulation. This indeed happens for the relatively slender block B10M, but not for the stockier blocks B6M and B2M, which raises concerns about appropriateness of η_{H} in real situations.

Furthermore, we have noticed that the designed set of tapes is not able to completely eliminate jumping for stocky blocks where $\frac{h}{b} \leq 1$ (see an example of such behaviour in Fig. 10). For this reason, only blocks with $\frac{h}{b} > 1$, for which no jumping is detected in the experiments, are analysed in the rest of this study.

To preliminarily test whether a constant coefficient of restitution is able to model rocking at all, we next try to find a "real" coefficient of restitution by running the simulation with a variety of restitution coefficients and

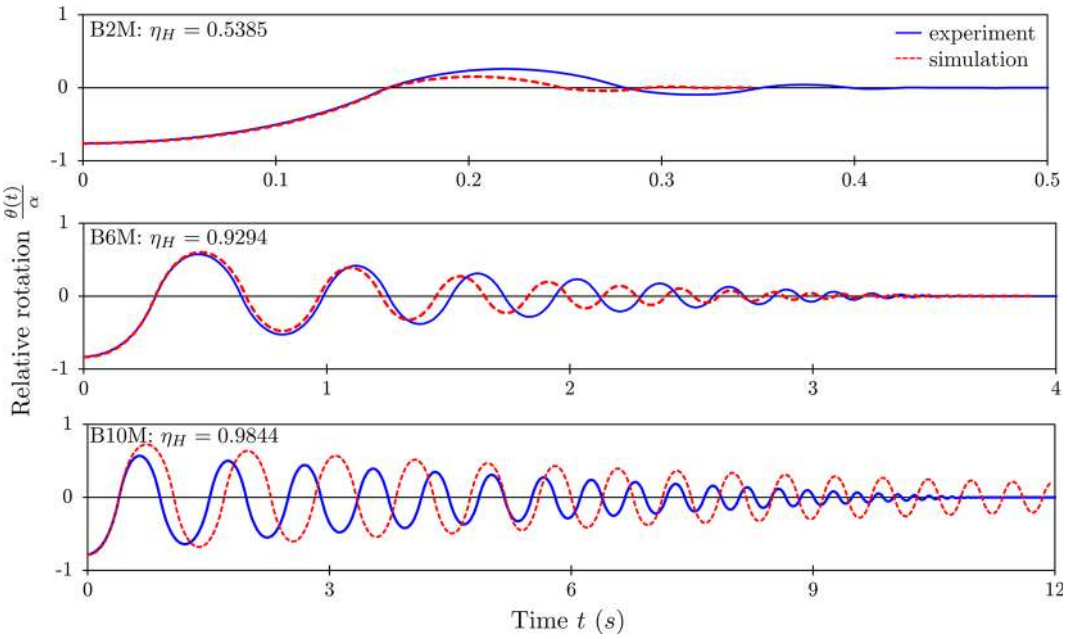

Fig. 9 Comparison between full-contact experiments and simulation using η_{H}

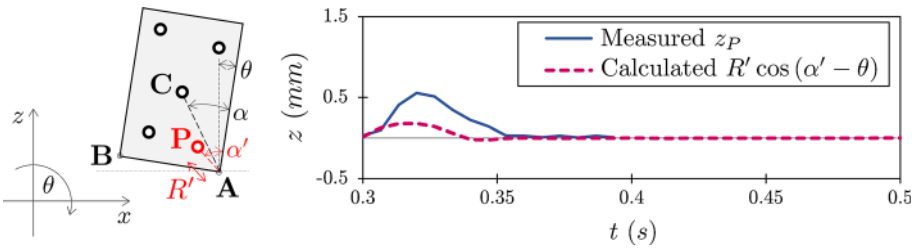

Fig. 10 Comparison between the measured and the calculated (from the assumption that only pure rocking takes place) coordinate z of a chosen point P on the stocky block B1L with $\frac{h}{b} = 1$

choosing the one which fits the experimental results best, which we denote as η_{e}. The best fitting is defined by the criterion that both the amplitudes and the periods of rocking fit graphically well during the middle 50% of the response. Figure 11 shows the corresponding results for block B2M, where the green dashed line shows the numerical results obtained by fitting the experimental results with a constant value of coefficient of restitution $\eta_{\mathrm{e}} = 0.67$ throughout the duration of rocking. Note that, as discussed earlier, for this block $\eta_{\mathrm{e}} > \eta_{\mathrm{H}}$. In order to assess to what extent the type of the tapes used affects the actual response, a number of tests have been repeated using a different tape (3M Micropore surgical tape instead of sellotape) and it has been found out that the coefficients η_{e} obtained for these two different tapes differ by less than 0.5%. A more elaborate analysis, not conducted within the course of this work, involving, e.g., fastening a block to the ground via a pre-stressed tendon set in order to ensure pure rocking, would be needed to provide a direct contact between the block and the ground and thus eliminate any impact the tape interface might have introduced.

The comparison between experimentally and numerically obtained energy time histories for block B2M in Fig. 11 shows that the assumption that energy loss is instantaneous at impacts can simulate the real energy loss sufficiently good. For this block, a constant value of coefficient of restitution models the experimental behaviour quite well.

However, not quite so good an agreement between the numerically and experimentally obtained results may be obtained by fitting the coefficient of restitution for significantly more slender blocks. This is illustrated for block B10M in Fig. 12. This figure indicates that *the restitution coefficient should not be assumed as constant* throughout the duration of free rocking. The green dashed line shows the results obtained using the coefficient of restitution η_{e} determined by fitting the overall response, and it is obvious that, in contrast to the results for block B2M, the experimentally observed changes in the rocking periods may not be accurately followed. To

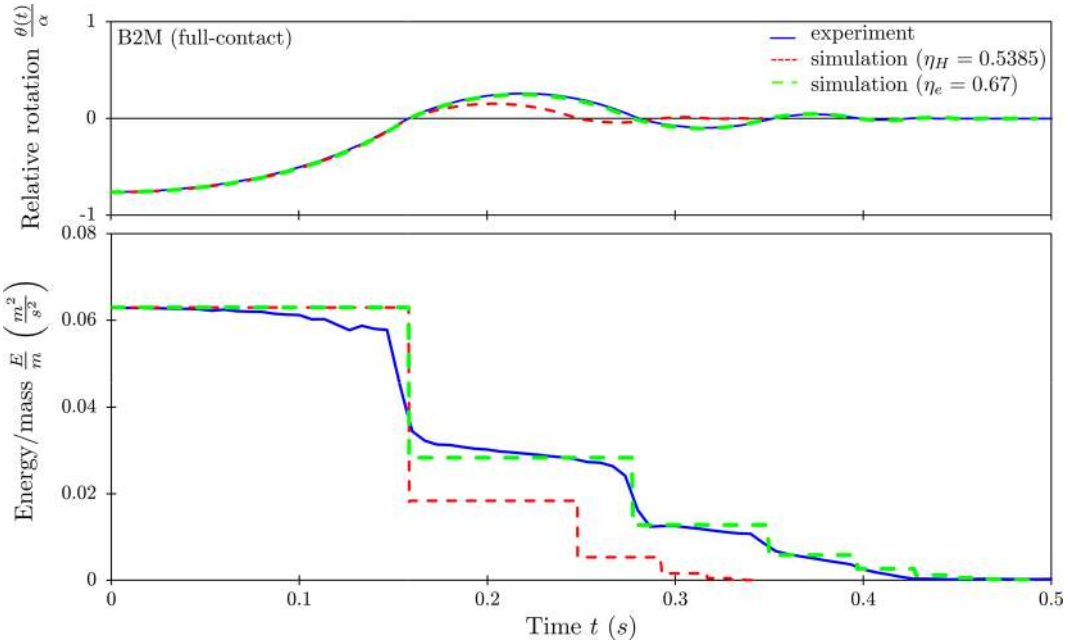

Fig. 11 Comparison between full-contact experiments and simulation using η_{H} and η_{e} for block B2M

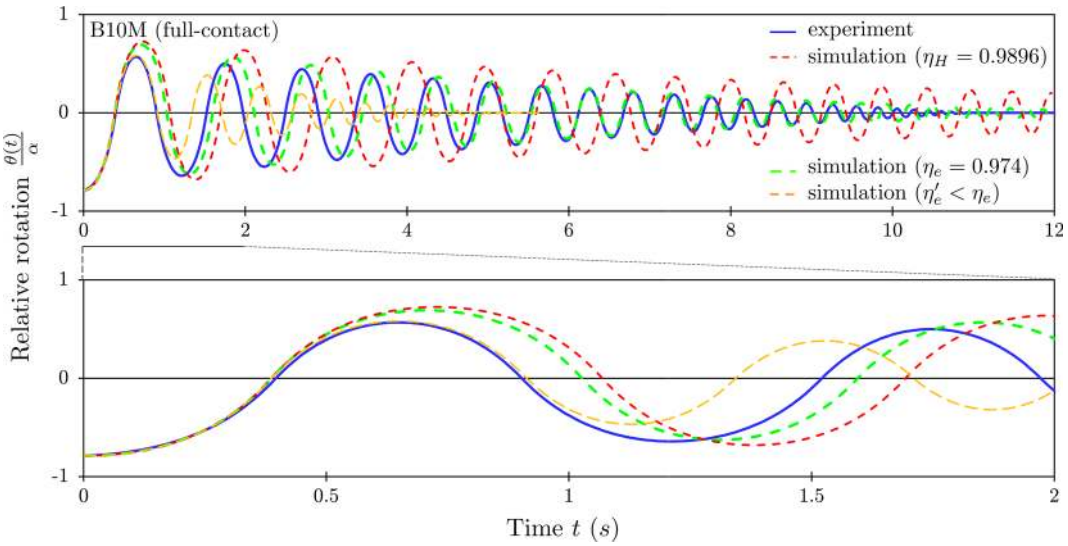

Fig. 12 Experimental and numerical results for block B10M and different restitution coefficients

gain more insight, we also show the results (the orange dashed line) for a coefficient of restitution η'_{e} obtained by fitting only the first post-impact half-period of rocking. The results are blown out for the first two seconds of motion in the lower part of Fig. 12.

If we take the difference between η_{e} and η'_{e} as a measure of variability of the restitution coefficient during rocking and repeat the analysis for ten different slenderness ratios (blocks B1M–B10M), we observe two interesting phenomena. Firstly, as already noted earlier, Housner's restitution coefficient η_{H} underestimates the actual restitution (i.e., overly dissipative) for stocky blocks, but the actual restitution for the analysed problems appears to be constant (see Fig. 13 for slenderness ratios below cca 4). Secondly, while for the relatively slender blocks (slenderness ratio above cca 6) Housner's restitution is now larger than the actual one (which is physically justified), the latter may not any more be considered as constant. Figure 13 shows that the difference between η_{e} and η'_{e} increases as the slenderness increases, in turn indicating an increase in

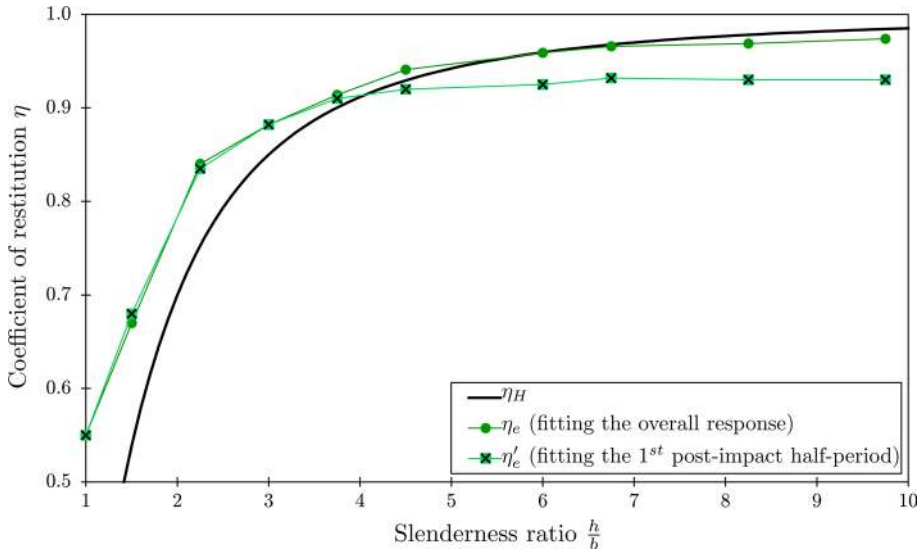

Fig. 13 Coefficient of restitution from Housner's formula [7] and full-contact experiments for blocks B1M–B10M (medium scale) with different fitting

Table 3 Coefficient of restitution $\eta_{e,full}$ from full-contact experiments

Block	$\eta_{e,full}$	Block	$\eta_{e,full}$	Block	$\eta_{e,full}$
B2S	0.690	B2M	0.670	B2L	0.708
B3S	0.825	B3M	0.840	B3L	0.852
B4S	0.890	B4M	0.882	B4L	0.904
B5S	0.919	B5M	0.914	B5L	0.937
B6S	0.948	B6M	0.941	B6L	0.952
B7S	0.958	B7M	0.959	B7L	0.970
B8S	0.960	B8M	0.966	B8L	0.972
B9S	0.964	B9M	0.969	B9L	0.978
B10S	0.966	B10M	0.974	B10L	0.979

variability of the actual restitution during rocking. As an estimate for the actual restitution we will from now on take η_e, as the one on the safe side when assessing stability of a block against overturning.

The inappropriateness of Housner's restitution estimate, especially for stocky blocks (which is way too liberal and thus unsuitable for design purposes), is also observed in the experiments performed on the other two scales in this work (see Table 3), as well as noticed by other researchers as shown in Fig. 14.

With the decrease in size of the block, η_H seems to describe restitution somewhat better—it overestimates the energy loss for slenderness ratios lower than 6 for scale S and lower than 8 for scale L.

5.2 Edge-contact experiments

To test whether the reason for unsuitability of Housner's restitution estimate applied to stocky blocks lies in an increased uncertainty in the position of the actual contact impulse as the slenderness decreases (as suggested by [4,8]), we will now repeat our analysis on a different set of suitably designed experiments. To this end, we provide different contact conditions in which this position may be determined much more accurately—the edge-contact conditions shown in Fig. 7.

The analysis with the edge-contact conditions is first repeated for block B2M. The results are shown in Fig. 15, along with those obtained earlier using the full-contact conditions. Clearly, in the case of edge contact, η_H enables a much better simulation than in the case of full contact. As noted above, this is expected since the edge-contact experiments provide conditions that are much closer to the assumptions of Housner's impact model. Still, η_H in this case slightly underestimates the actual restitution (see inset in Fig. 15) and analysis will be performed next to see whether Housner's estimate may be improved following [4,8].

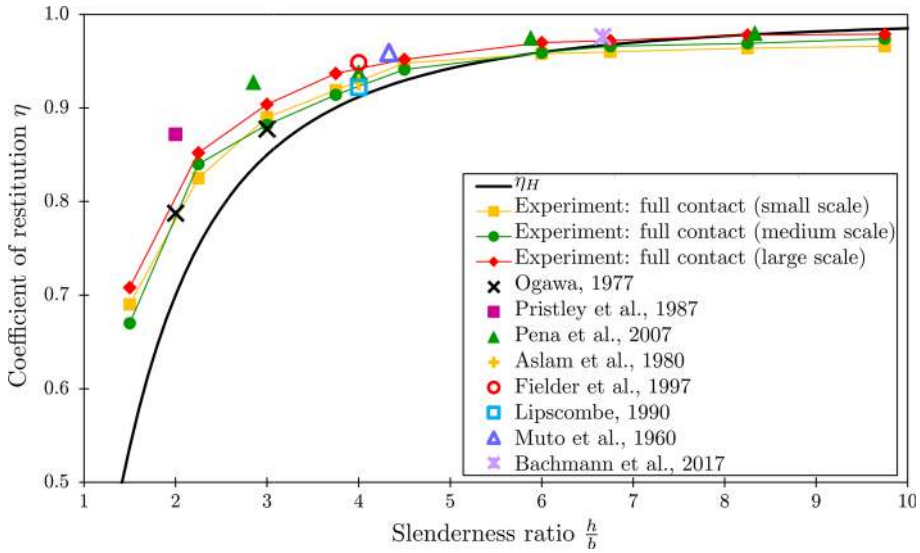

Fig. 14 η_{H} [7] and coefficient of restitution obtained from full-contact experiments [2,3,6,9,15–18]

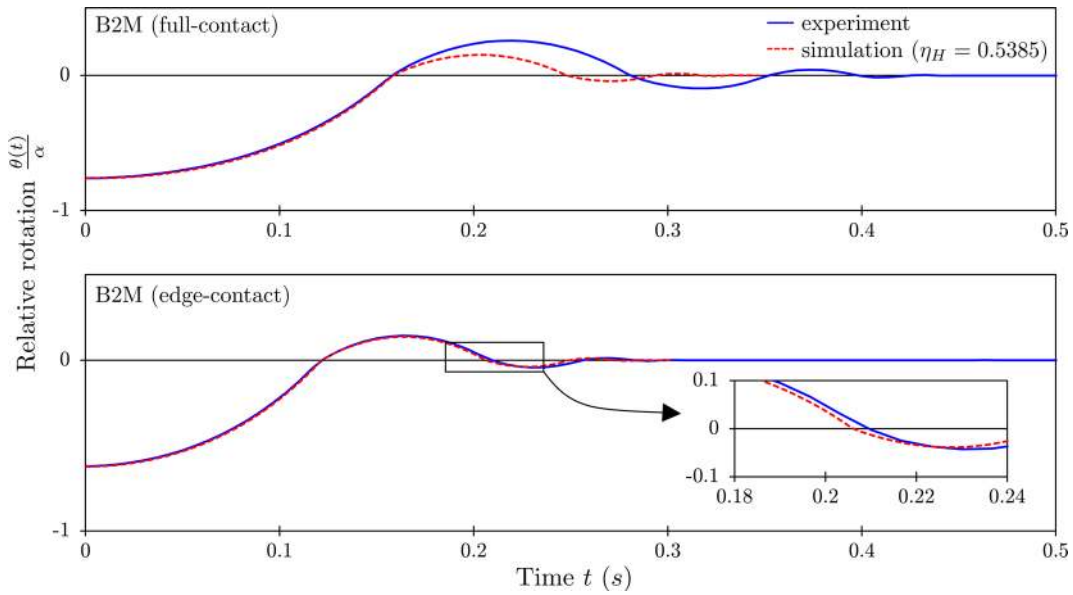

Fig. 15 Experimental and numerical results for block B2M and different contact conditions

The two series of experiments have been carried out for all the blocks from B1S to B10L. For the purpose of comparison between experimentally and numerically obtained results, the experimentally obtained coefficient of restitution η_{e} is used for all the blocks, i.e., the coefficient of restitution calculated by fitting the numerical curve to the experimentally obtained one over the whole response time. The results for the blocks of width 4.5 cm (medium scale) and both full- and edge-contact conditions are given in Fig. 16, which shows a very significant effect of the size of the contact area on the restitution during free rocking.

Below, the results are presented with respect to block's slenderness $\frac{h}{b}$ separately for each of the three scales. If the contact is assumed to take place between the block and the inner edge of the base ($l_c = 1.5$ mm in Table 4), we can compute the upper bound for the restitution coefficient of [4,8]. On the other hand, the contact can be assumed to take place midway between the inner edge of the base and the edge of the block, in which case $l_c = \frac{1.5}{2}$ mm. Parameters k necessary to compute η_{M} obtained from these two approaches using (14) are given in Table 4 for the three scales.

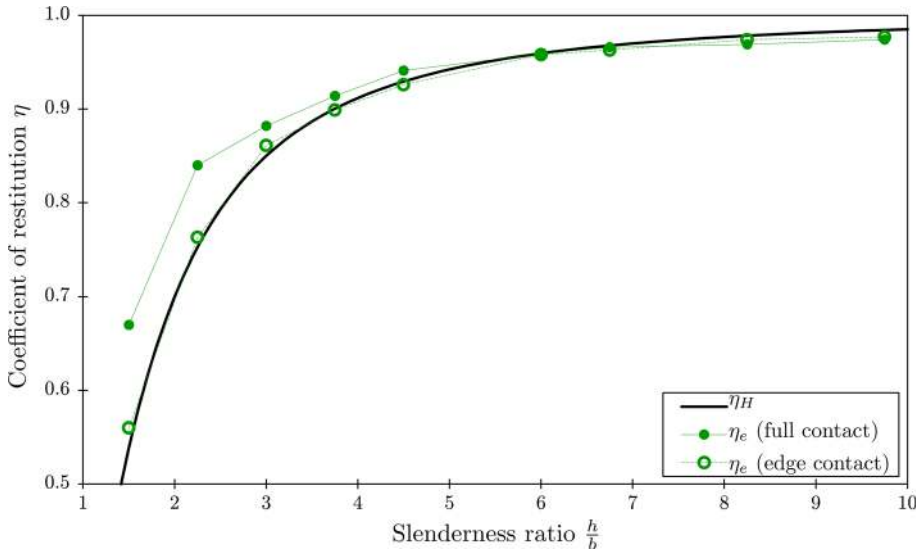

Fig. 16 Experimentally obtained results from full- and edge-contact experiments (medium scale, $b = 4.5\,\text{cm}$)

Table 4 Values of the parameter k in edge-contact experiments

	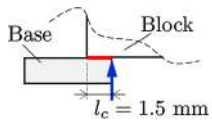	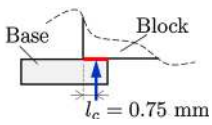
Scale	k_1	k_2
SMALL	0.9	0.95
MEDIUM	$0.9\dot{3}$	$0.9\dot{6}$
LARGE	0.95	0.975

The experimentally obtained results for blocks B1S–B10S from Table 2 are shown in Fig. 17. The coefficients η_H is shown with the full black line, which clearly underestimates block's restitution for slenderness ratio lower than 4.5, while η_M calculated using $k = 0.9$ and $k = 0.95$ give improved estimates which are almost always higher than the corresponding values from the edge-contact experiments for all the slenderness ratios analysed.

The corresponding results for blocks B1M to B10M are shown in Fig. 18. The coefficients η_H again underestimates the restitution for slenderness ratios lower than 4.5. The coefficients η_M with $k = 0.9\dot{3}$ and $k = 0.9\dot{6}$ again almost always return higher restitution estimates than those experimentally obtained for all the slenderness ratios.

Likewise, the results for blocks B1L to B10L are shown in Fig. 19. For this largest scale, η_H overestimates the energy loss for slenderness ratios lower than 3. In contrast, coefficients η_M calculated with $k = 0.95$ and $k = 0.975$ are higher than those experimentally obtained for the complete range of slenderness ratios analysed.

Clearly, the results in Figs. 17, 18 and 19 show that Housner's restitution estimate is much more suitable when we know that the impact actually takes place near the edge of the block. In addition, they show that the modified restitution estimate given in [4,8] for the position of the impact as away from the edge of the block as applicable is always higher than that experimentally observed and may be thus taken to be the upper limit of the restitution coefficient. In practical situations, however, this position is unknown and in the following we suggest a method to determine it.

5.3 Estimate of material dissipation from edge-contact experiments

An analysis is now performed so that an insight into the additional energy loss due to material dissipation is provided: the ratio between the experimentally obtained restitution η_e and the η_M from (14) should provide a

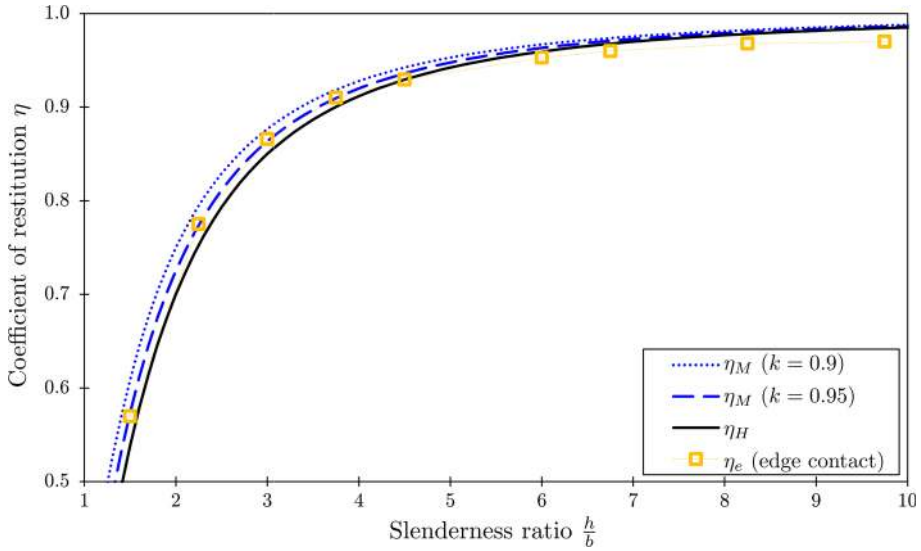

Fig. 17 Coefficient of restitution for blocks B1S–B10S (small scale, $b = 3$ cm) with full- and edge-contact conditions

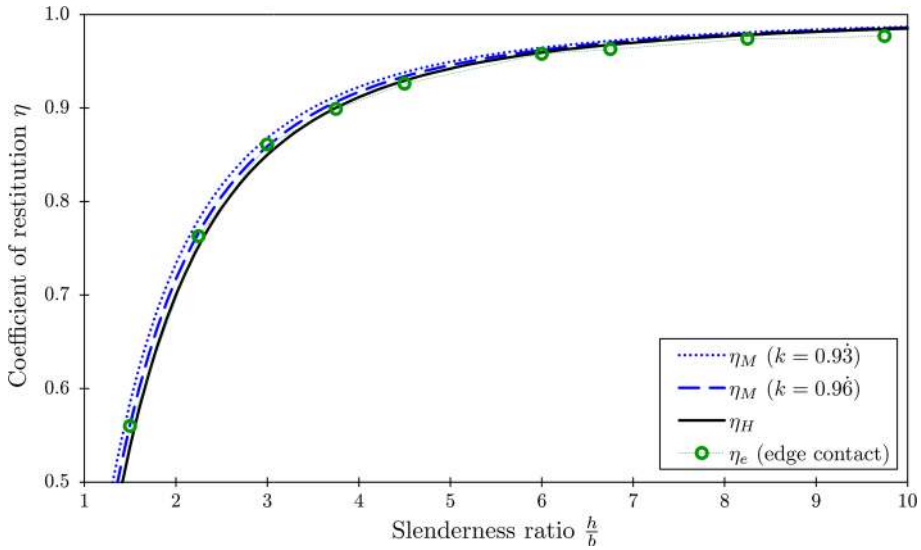

Fig. 18 Coefficient of restitution for blocks B1M–B10M (medium scale, $b = 4.5$ cm) with full- and edge-contact conditions

quantitative information about material dissipation:

$$\eta_{\text{mat}} = \frac{\eta_{\text{e}}}{\eta_{\text{M}}} \Leftrightarrow \eta_{\text{e}} = \eta_{\text{M}}\eta_{\text{mat}} \tag{16}$$

and from Figs. 17, 18 and 19 we expect that for the edge-contact experiments η_{mat} obtained in this way should be approximately constant.

The ratio between the experimentally obtained restitution η_{e} and the corresponding η_{M} is plotted in Fig. 20 taking into account the two approaches from Table 4 for all the edge-contact experiments carried out. This ratio is near-constant for the slenderness ratio higher than 3 if we assume that the contact takes place at the inner edge of the base ($\eta_{\text{mat}} = \frac{\eta_{\text{e}}}{\eta_{\text{M}}} \simeq 0.989$), which indicates that η_{M} gives consistent results for such geometries and contact conditions. On the other hand, this ratio is near-constant for all the observed slendernesses if we assume that the contact takes place midway between the inner edge of the base and the edge of the block ($\eta_{\text{mat}} = \frac{\eta_{\text{e}}}{\eta_{\text{M}}} \simeq 0.994$), but in this case it reaches unacceptable values higher than 1 for slenderness ratios between 2 and 4 on scale S, as well as for slenderness ratio 3 on scale M. This indicates that the contact point has to be assumed further from the edge of the block.

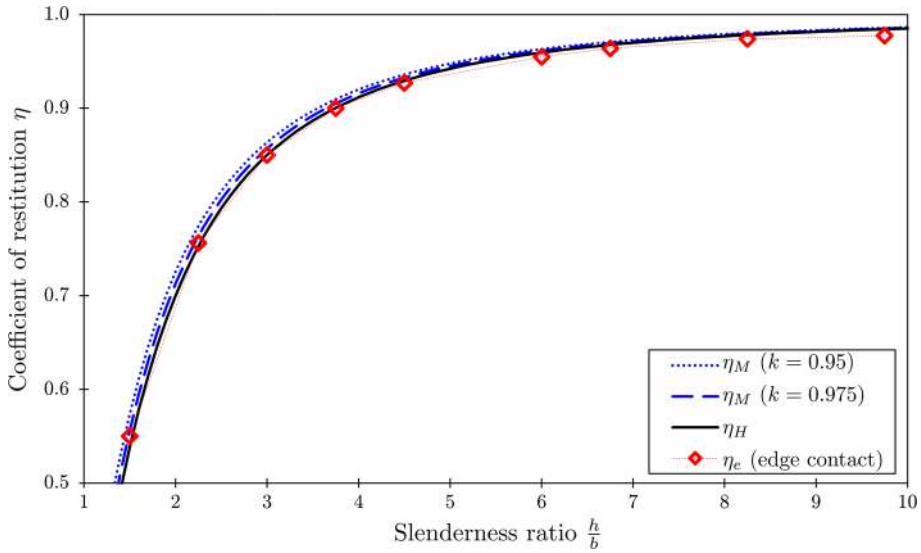

Fig. 19 Coefficient of restitution obtained for blocks B1L–B10L (large scale, $b = 6$ cm) with full- and edge-contact conditions

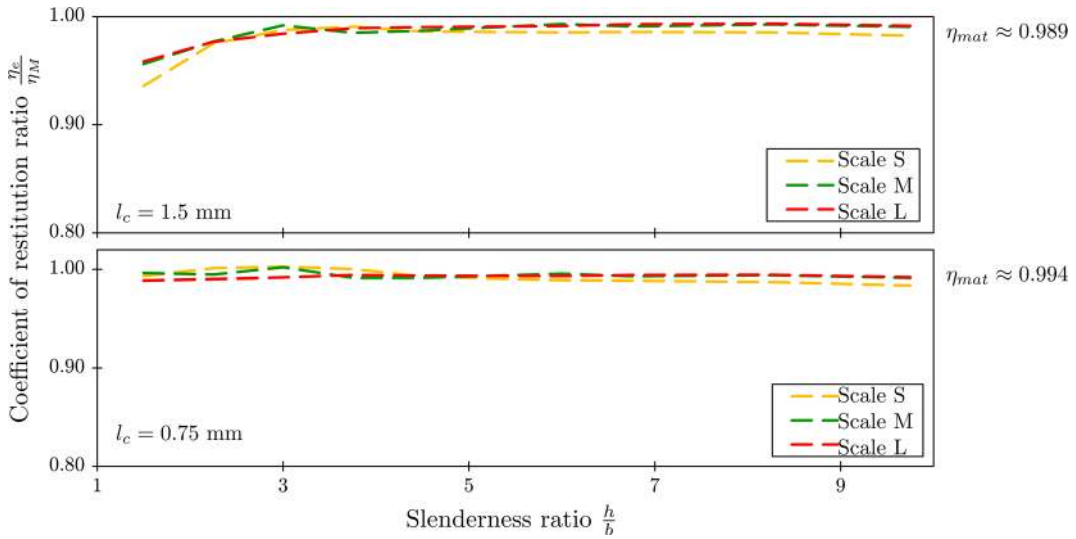

Fig. 20 Ratio between the experimentally obtained coefficient of restitution η_e and η_M [4,8] for the edge-contact experiments

The approach where the contact is assumed to take place on the inner edge of the base is on the safe side, and it is clearly to be preferred.

5.4 Inverse analysis for assessment of k in (14) for full-contact experiments

Since generally we are not able to detect the point at which the contact takes place in full-contact experiments, here we suggest an inverse analysis which enables assessment of the approximate values k (and thus also the contact point) for the full-contact rocking conditions. Fundamentally, η_{mat} is assumed to be purely a measure of material dissipation, not dependent on contact conditions. Then, its value calculated from the edge-contact experiments is also valid for the full-contact conditions, which supplies an estimate for the amount of rigid-body restitution η_{RB} in the full-contact experiments:

$$\eta_{\text{mat}} = \frac{\eta_{\text{e,full}}}{\eta_{\text{RB}}} \rightarrow \eta_{\text{RB}} = \frac{\eta_{\text{e,full}}}{\eta_{\text{mat}}}. \tag{17}$$

Table 5 Parameter k in (14) and position $\overline{b}$ of the contact impulse in Fig. 2 for $\eta_{\text{mat}} = 0.989$ for the full-contact experiments

Block	Scale S		Scale M		Scale L		Average k
	k	$\overline{b}$	k	$\overline{b}$	k	$\overline{b}$	
B2	0.7704	0.0116	0.8805	0.0180	0.7429	0.0223	0.7713
B3	0.8001	0.0120	0.7595	0.0171	0.7259	0.0218	0.7619
B4	0.8059	0.0121	0.8397	0.0189	0.7440	0.0223	0.7965
B5	0.8364	0.0125	0.8670	0.0195	0.7175	0.0215	0.8070
B6	0.7602	0.0114	0.8241	0.0185	0.7214	0.0216	0.7685
B7	0.8766	0.0131	0.8621	0.0194	0.6838	0.0205	0.8075
B8	0.9526	0.0143	0.8468	0.0191	0.7266	0.0218	0.8420
B9	1.0787	0.0162	0.9634	0.0217	0.7121	0.0214	0.9181
B10	1.2214	0.0183	0.9838	0.0221	0.8016	0.0240	0.9181
Average	0.9003	0.0135	0.8608	0.0194	0.7306	0.0219	0.8306

Bearing in mind that η_{M} in (14) is also a coefficient of rigid-body restitution but such one computed from the angular momentum balance in which k is the parameter defining the position of the resultant contact impulse, substituting η_{RB} for η_{M} in (14) provides a result for this position as

$$k = \sqrt{\frac{(1-\eta_{\text{RB}})\left(4-3\sin^2\alpha\right)}{(1+\eta_{\text{RB}})\,3\sin^2\alpha}}, \quad \overline{b} = \frac{b}{2}k, \tag{18}$$

where $\overline{b}$ is shown in Fig. 2. The values of the parameter k and the position $\overline{b}$ for each block obtained in this way are given in Table 5. Note that the values for k and $\overline{b}$ for blocks B9S and B10S obtained in this way are larger than the maximum possible values ($k = 1$, $\overline{b} = b/2$; see Fig. 2). We suggest that this occurs due to the system of tapes designed to prevent jumping and sliding: the tapes act as an additional dissipation mechanism which has the biggest influence on the smallest scale due to the smallest mass of the block. This additional dissipation cannot be fully taken into account with η_{mat} obtained as the average of $\eta_{\text{e}}/\eta_{\text{M}}$ in Sect. 5.3 over all scales and slendernesses.

The results for average k for each scale (S, M and L) indicate that k decreases with an increase in size of the blocks, which means that the position of impact impulse moves towards the centre of the block with an increase in block's size.

The assumed constant value of k models the experiment very well for the largest scale, as shown in Fig. 21. However, with the decrease in scale there is an increasing difference between η_{M} and η_{RB} which indicates that the value k is increasingly related to the slenderness of the block as size decreases.

The proposed approach is not limited to blocks of a given size or slenderness (see Sect. 5.5 below), but the results obtained do follow from a set of specific experiments conducted on a given combination of contact materials (here, aluminium to aluminium; the material of the tape used has little effect on the results, as stated in Sect. 5.1). For different materials of the block or the base, the experimental program should be repeated using appropriate specimens made of the new material.

5.5 Application to blocks of arbitrary size and slenderness

The results in the above study indicate that the parameter k in η_{M} (14) is a function of both slenderness and size of a block, and an attempt is made here to obtain a mathematical dependence of k on these geometric properties.

The experimental results collected (involving three different sizes and nine different slendernesses) have been used as the input for a linear–quadratic fit by the method of least-squares, which has resulted in the following formula:

$$k\left(\frac{h}{b}, b\right) = 0.0047\left(\frac{h}{b}\right)^2 - 0.0258\frac{h}{b} + 1.0635 - 0.0565b, \tag{19}$$

where b is to be input in cm. The surface $k\left(\frac{h}{b}, b\right)$ is plotted in Fig. 22.

To test this result, a larger additional block B6XL with $b = 0.09\,\text{m}$, $h = 0.405\,\text{m}$ (so $h/b = 4.5$) and $m = 8716.8\,\text{g}$ is tested in free rocking. For this block, formula (19) gives $k = 0.7036$, the restitution coefficient

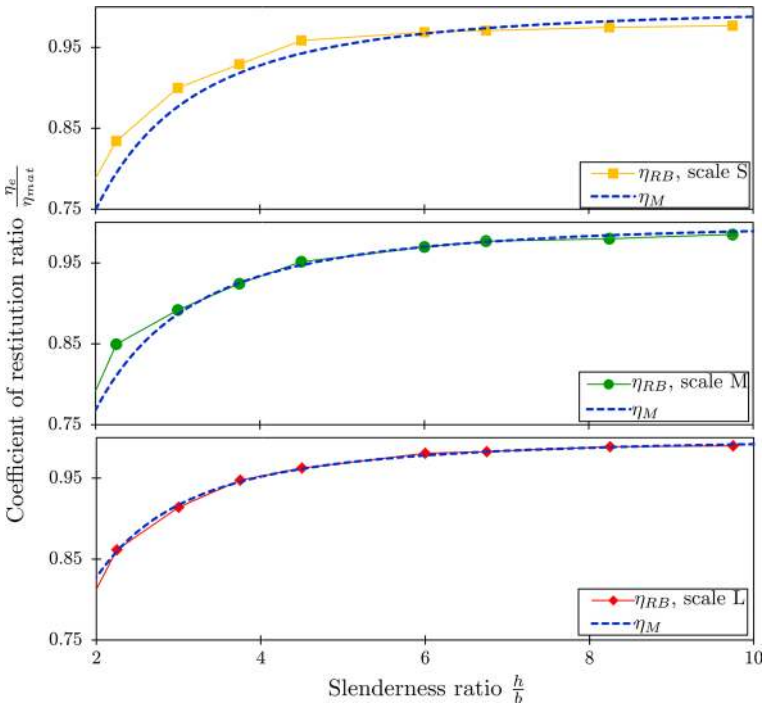

Fig. 21 Coefficient of restitution η_{RB} and η_{M} [4,8]

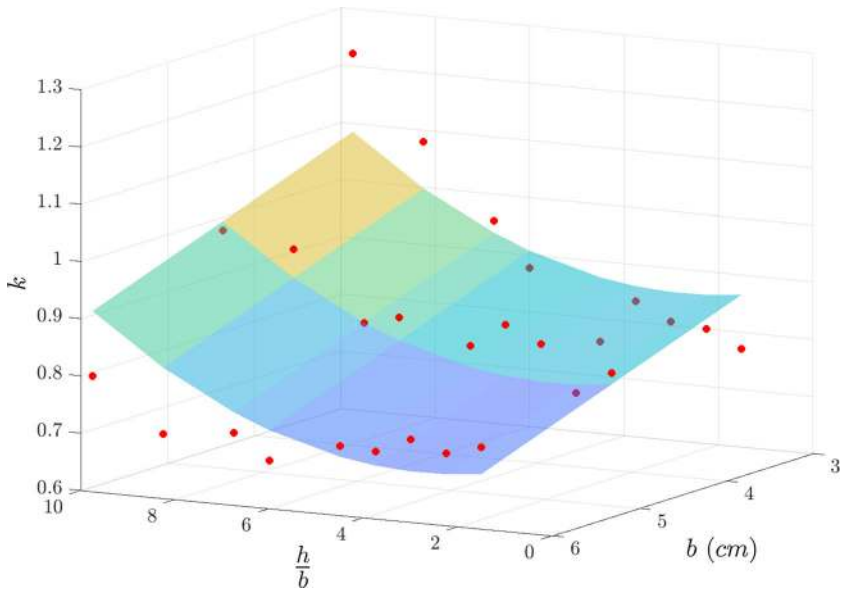

Fig. 22 Least-square prediction for k

thus following from (14) as $\eta_{\mathrm{M}} = 0.9644$. The results from a simulation run using this restitution coefficient as input are shown in Fig. 23, along with the experimental measurements, and a simulation using Housner's restitution. Obviously, the simulation using k from (19) fits the experiment quite well.

Still, it needs to ba stressed that the experimental programme has been limited to only three different block sizes (S, M, L) and validated against a single additional size (XL). Consequently, the presented result has to be understood only as a promising guidance towards devising an estimate for k. The presented research needs to be tested against additional significantly larger blocks to provide a definite estimate for k and η_{M}.

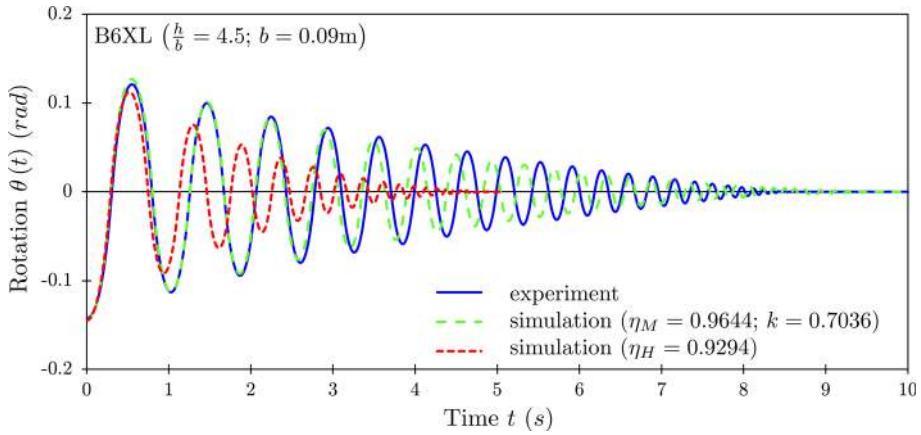

Fig. 23 Rotation time history obtained experimentally and numerically with η_{H} and η_{M} using k obtained from (19)

6 Conclusions and future work

This paper discusses the dynamic response of single rigid prismatic blocks in free rocking without sliding and jumping treated numerically and experimentally. The emphasis is put on the analysis of the post-impact behaviour and energy loss mechanism during impacts. To enable analysis of both slender and stocky blocks in large-amplitude rocking, full nonlinearity of the rocking behaviour is taken into account in the numerical simulations. A time-stepping numerical procedure is developed with built-in contact detection algorithm, which enables a precise investigation of energy loss during impact. Two different impact models and restitution estimates are considered: Housner's classical model (η_{H}) [7] and the improved model (η_{M}) given by Kalliontzis et al. [8] and Chatzis et al. [4].

An extensive controlled experimental study of free rocking behaviour with ten different slenderness ratios, three scales (sizes) and two different contact conditions which prevent sliding and jumping is conducted. The comparisons between the experimentally and numerically obtained results show that bouncing back and remaining still after the impact is unlikely to occur in reality because it is not easy to completely prevent detachment of stocky blocks from the ground. The restitution coefficient is shown to change during rocking, but the overall response can still be modelled with sufficient accuracy with a constant restitution coefficient.

Housner's restitution coefficient η_{H} is widely reported to overestimate the energy loss and should be used with caution in seismic stability assessment, especially for stocky blocks, which is confirmed by the present analysis. The numerical results obtained using the improved restitution coefficient η_{M} due to Kalliontzis et al. and Chatzis et al. are in much better agreement with the experimentally obtained values. Their suggestion that the impact between the block and the base takes place at some point between the corners of the block is verified with experiments where the contact between the block and the base is designed so that the actual contact region is controlled and known (the edge-contact experiments).

In addition, an approach for estimating restitution due to material dissipation η_{mat} and the position of the contact point in full-contact experiments is presented. With this position known, the corresponding improved restitution [4,8] models the full-contact rocking behaviour significantly better than Housner's model and provides an accurate estimate of the energy loss in rocking, which is always on the conservative side and thus suitable for assessment of rocking stability. Finally, a suggestion for devising an estimate for the coefficient k for a block of arbitrary size and slenderness is given.

Based on the present results, further numerical and experimental analysis of rocking due to an arbitrary base acceleration function will be conducted in the future. The procedure will be also generalised to a dual-block stack so that the conditions for complete or partial overturning may be investigated.

Acknowledgements The results presented in this work have been obtained within the research project *Configuration-dependent approximation in non-linear finite-element analysis of structures* financially supported by the Croatian Science Foundation under Contract No. HRZZ-IP-11-2013-1631. The laboratory equipment used in this research is purchased within the project *Research Infrastructure for University of Rijeka Campus (RISK)* funded by the European Fund for Regional Development.

References

1. Acary, V.: Projected event-capturing time-stepping schemes for nonsmooth mechanical systems with unilateral contact and Coulomb's friction. Technical report. INRIA, Grenoble, Rhone-Alpes (2012)
2. Aslam, M., Scalise, D.T., Godden, W.G.: Earthquake rocking response of rigid bodies. J. Struct. Div. **106**(2), 377–392 (1980)
3. Bachmann, J.A., Strand, M., Vassiliou, M.F., Broccardo, M., Stojadinović, B.: Is rocking motion predictable? Earthq. Eng. Struct. Dyn. **42**(2), 535–552 (2017)
4. Chatzis, M.N., Garcia Espinosa, M., Smyth, A.W.: Examining the energy loss in the inverted pendulum model for rocking bodies. J. Eng. Mech. **143**(5), 04017013 (2017)
5. Dimitrakopoulos, E.G., DeJong, M.J.: Revisiting the rocking block: closed-form solutions and similarity laws. Proc. R. Soc. A Math. Phys. Eng. Sci. **468**(2144), 2294–2318 (2012)
6. Fielder, W., Virgin, L., Plaut, R.: Experiments and simulation of overturning of an asymmetric rocking block on an oscillating foundation—Scholars@Duke. Eur. J. Mech. A Solids **16**(5), 905–923 (1997)
7. Housner, G.W.: The behavior of inverted pendulum structures during earthquakes. Bull. Seismol. Soc. Am. **53**(2), 403–417 (1963)
8. Kalliontzis, D., Sritharan, S., Schultz, A.: Improved coefficient of restitution estimation for free rocking members. J. Struct. Eng. **142**(12), 06016002 (2016)
9. Lipscombe, P.R.: Dynamics of rigid block structures. Ph.D. thesis, University of Cambridge (1990)
10. Ma, Q.T.M., Ming, Q.T.: The mechanics of rocking structures subjected to ground motion. Ph.D. thesis, The University of Auckland https://researchspace.auckland.ac.nz/handle/2292/5861 (2010)
11. Makris, N.: A half-century of rocking isolation. Earthq. Struct. **7**(6), 1187–1221 (2014)
12. Makris, N., Konstantinidis, D.: The rocking spectrum and the shortcomings of design guidelines. Technical report, Department of Civil and Environmental Engineering, University of California, Berkeley (2001)
13. Makris, N., Roussos, Y.: Response and overturning of equipment under horizontal pulse-type motions. Technical report, University of California, Berkeley (1998)
14. Makris, N., Zhang, J.: Rocking response and overturning of anchored equipment under seismic excitations. Technical report, University of California, Berkeley (1999)
15. Muto, K., Umemura, H., Sonobe, Y.: Study of the overturning vibrations of slender structures. In: Proceedings of the 2nd World Congress Earthquake Engineering, pp. 1239–1261 (1960)
16. Ogawa, N.: A study on rocking and overturning of rectangular column. Technical report, National Research Center for Disaster Prevention (1977)
17. Peña, F., Prieto, F., Lourenço, P.B., Campos-Costa, A., Lemos, J.V.: On the dynamics of rocking motion of single rigid-block structures. Earthq. Eng. Struct. Dyn. **36**(15), 2383–2399 (2007)
18. Priestley, M.J.N., Evison, R.J., Carr, A.J.: Seismic response of structures free to rock on their foundations. Bull. N. Z. Natl. Soc. Earthq. Eng. **11**(3), 141–150 (1978)
19. Shi, B., Anooshehpoor, A., Zeng, Y., Brune, J.N.: Rocking and overturning of precariously balanced rocks by earthquakes. Bull. Seismol. Soc. Am. **86**(5), 1364–1371 (1996)
20. Smoljanović, H., Živaljić, N., Nikolić, Ž.: A combined finite-discrete element analysis of dry stone masonry structures. Eng. Struct. **52**, 89–100 (2013). https://doi.org/10.1016/j.engstruct.2013.02.010
21. Spanos, P.D., Koh, A.S.: Rocking of rigid blocks due to harmonic shaking. J. Eng. Mech. **110**(11), 1627–1642 (1985)
22. Wilson, E.L.: Three-Dimensional Static and Dynamic Analysis of Structures, 3rd edn. Computers and Structures, Inc., Berkeley (2002)
23. Zhang, J., Makris, N.: Rocking response of free-standing blocks under cycloidal pulses. J. Eng. Mech. **127**(5), 473–483 (2001)